Hindawi
Wireless Communications and Mobile Computing
Volume 2018, Article ID 2870518, 15 pages
https://doi.org/10.1155/2018/2870518

Research Article

Fuzzy Based Network Assignment and Link-Switching Analysis in Hybrid OCC/LiFi System

Moh. Khalid Hasan, Mostafa Zaman Chowdhury, Md. Shahjalal, and Yeong Min Jang

Department of Electronics Engineering, Kookmin University, Seoul 02707, Republic of Korea

Correspondence should be addressed to Yeong Min Jang; yjang@kookmin.ac.kr

Received 3 August 2018; Accepted 4 November 2018; Published 19 November 2018

Academic Editor: Laurie Cuthbert

In recent times, optical wireless communications (OWC) have become attractive research interest in mobile communication for its inexpensiveness and high-speed data transmission capability and it is already recognized as complementary to radio-frequency (RF) based technologies. Light fidelity (LiFi) and optical camera communication (OCC) are two promising OWC technologies that use a photo detector (PD) and a camera, respectively, to receive optical pulses. These communication systems can be implemented in all kinds of environments using existing light-emitting diode (LED) infrastructures to transmit data. However, both networking layers suffer from several limitations. An excellent solution to overcoming these limitations is the integration of OCC and LiFi. In this paper, we propose a hybrid OCC and LiFi architecture to improve the quality-of-service (QoS) of users. A network assignment mechanism is developed for the hybrid system. A dynamic link-switching technique for efficient handover management between networks is proposed afterward which includes switching provisioning based on user mobility and detailed network switching flow analysis. Fuzzy logic (FL) is used to develop the proposed mechanisms. A time-division multiple access (TDMA) based approach, called round-robin scheduling (RRS), is also adopted to ensure fairness in time resource allocation while serving multiple users using the same LED in the hybrid system. Furthermore, simulation results are presented taking different practical application scenarios into consideration. The performance analysis of the network assignment mechanism, which is provided at the end of the paper, demonstrates the importance and feasibility of the proposed scheme.

1. Introduction

Communication currently relies on the radio-frequency (RF) spectrum, which is overcrowded and strictly regulated [1]. Because of several factors including interference, limited resources, and human safety it is obvious that RF based technologies will not be sufficient to manage the massive future data traffic. Wireless communication using the optical spectrum has been regarded as a congruent solution to the spectrum congestion of RF based technologies [2–6]. In particular, the optical wireless technology, especially visible light communication (VLC), has added a new dimension in the world of mobile communications for its huge unregulated spectrum (up to 800 THz [7]), cost effectiveness, energy efficiency, and high security [3, 8, 9]. Moreover, current indoor and outdoor environments are currently heavily congested with light-emitting diode (LED) based lighting infrastructures, enabling VLC to be exploited as a complementary technology to RF.

Light fidelity (LiFi) is a subset of OWC technology in which a photo detector (PD) receives the variation in the intensity of light, which carries data bits encoded from the light source [3, 10, 11]. A PD can detect high-speed LED flickering, a capability that enables LiFi to support high data rates. An extensive improvement in bandwidth reuse is observed for LiFi technologies, resulting in excellent spectral efficiency. Because of these benefits provided by LiFi, several architectures integrating LiFi and RF have been already proposed to enhance the quality-of-service (QoS) of users; these architectures include those that manage resource allocation [12–15], dynamic handover [16, 17], energy harvesting [18], delay analysis [19], and channel assignment [20].

However, LiFi cannot be efficiently utilized in daylight because it suffers from extensive interference generated by sunlight [3]. In indoor environments, it can suffer from the same problem resulting from neighboring lighting infrastructures. LiFi has a low signal-to-interference-plus-noise ratio (SINR) because it is heavily affected by the interferences generated by adjacent light sources. In addition, the communication distance that can be obtained using LiFi is comparatively short with respect to other existing technologies. These limitations inspire further research on the optimum potentiality of LiFi in practical environments.

Optical camera communication (OCC) is a recently introduced VLC technique that uses an image sensor to receive optical signals [21–26]. The exponential growth in camera-mounted smart devices has enabled OCC to be utilized in innovative application scenarios, such as indoor/outdoor positioning [27, 28], localized advertising [29], digital signage, and vehicle-to-vehicle (V2V) or vehicle-to-infrastructure (V2I) communications [30–32]. OCC has added significant user flexibility with the use of smartphone cameras to receive data from LEDs. Furthermore, OCC is highly stable in terms of variations in communication distance. Because of the limited angle-of-view (AoV) of cameras, OCC is less affected by interferences generated from neighboring LEDs. However, similar to LiFi, OCC has several limitations. For example, because of the meager sampling rates of current commercial cameras, OCC offers a low data rate, which particularly decreases the user QoS.

Until now, a hybrid OCC and LiFi model had not been developed. In this study, a hybrid networking architecture integrating OCC and LiFi is proposed to enhance the user QoS. The network is assigned to users through utilization of fuzzy logic (FL). FL is a convenient approach to map an input to an output and is provided on the basis of several truth scores ranging from 0 to 1 [33]. This method is flexible and intuitive without far-reaching complexity, which are characteristics that lead us to choose this approach. We propose a new network assignment mechanism inside the LED cell (the entire coverage area of the LED) for users. Fuzzy inputs are chosen using the parameters that determine the quality of both networks. The fuzzy rules are generated by considering real-world application scenarios of users. The center-of-gravity (CoG) method is used to defuzzify the inputs and obtain mark allocations for each user. Furthermore, we develop a FL-based vertical link-switching mechanism between the networking layers, as both of the networks support user mobility. We briefly discuss the switching probability and corresponding network switching flow analysis of the hybrid system. Round-robin scheduling (RRS) [34], an existing time-division multiple access (TDMA) approach, is adopted to ensure fairness in resource allocation among users.

The remainder of the paper is organized as follows: Section 2 provides a system overview and an analysis on channel parameters, which includes theoretical representations of SINR for both technologies. The FL-based network assignment mechanism, including a discussion on user QoS, is explained in Section 3. Sections 4 and 5 describe the link-switching strategy and the network switching flow process, respectively. The performance of the assignment mechanism is evaluated in Section 6, which also includes a discussion of the outage probability and QoS performance. A brief summary of our work is provided in Section 7. Finally, Section 8 presents future research possibilities related to our proposed hybrid infrastructure.

2. System Overview

2.1. Hybrid System Architecture. In this study, a hybrid OCC/LiFi networking layer is considered. Taking user mobility into account, this hybrid system can serve multiple users. Therefore, the hybrid system is suitable for any roaming or stationary user. A particular LED is configured by two parallel LED-driving circuitries. Although both technologies use the same optical spectrum, no interference will be generated because the TDMA based RRS method is exploited to allocate time resources when there are multiple users. A generalized block diagram of our proposed architecture is shown in Figure 1. The PD can receive high-rate LED flickering, whereas a camera cannot. Current commercial cameras are configured with low frame rates (in most cases, 30–50 frames per second). This configuration particularly reduces the modulation bandwidth of OCC [35, 36]. It is also worth noting that the LED flickering must not be observed by human eyes (equivalent to a threshold of approximately 100 Hz [37]).

2.2. OCC Channel Model. For a VLC system, the route for optical signal transmission has two components: line-of-sight (LOS) and non-line-of-sight (NLOS). Because of the nature of camera pixels, region-of-interest (RoI) mechanisms are applied for OCC, by which the reflection component of the transmitted signal is spatially separated from the LOS component [23]. An indoor hybrid system with the transmitter and receiver presented at T_x and R_x, respectively, is illustrated in Figure 2. The LED cell represents the entire coverage area of the LED.

The LOS channel for optical signal transmission is modeled by Lambertian radiant intensity, which is represented by the following equation [38]:

$$R_o(\alpha) = \frac{(m_l + 1)\cos^{m_l}(\alpha_{ir})}{2\pi} \tag{1}$$

where α_{ir} signifies the angle of irradiance of the LED. m_l is the Lambertian emission index, which originates from the radiation angle $\Psi_{1/2}$, called the radiation semiangle of the LED; m_l is defined as

$$m_l = -\log_{\cos\Psi_{1/2}} 2 \tag{2}$$

We assume that the Euclidean distance between T_x and R_x is $d_{a,b}$, which is calculated from the horizontal distance $d_{b,x}$ and the vertical distance $d_{a,h}$ ($d_{a,b} = \sqrt{d_{a,h}^2 + d_{b,x}^2}$). The overall DC channel gain for OCC is formulated as [12]

$$H_{t,r}^{IS} = g_{op}\cos(\alpha_{in})\,\Delta_{occ}\frac{R_o(\alpha)\,A_c}{d_{a,b}^2} \tag{3}$$

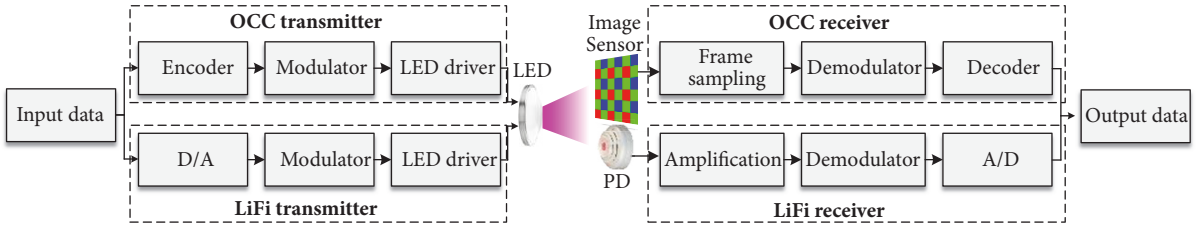

Figure 1: Basic block diagram of the hybrid OCC/LiFi architecture.

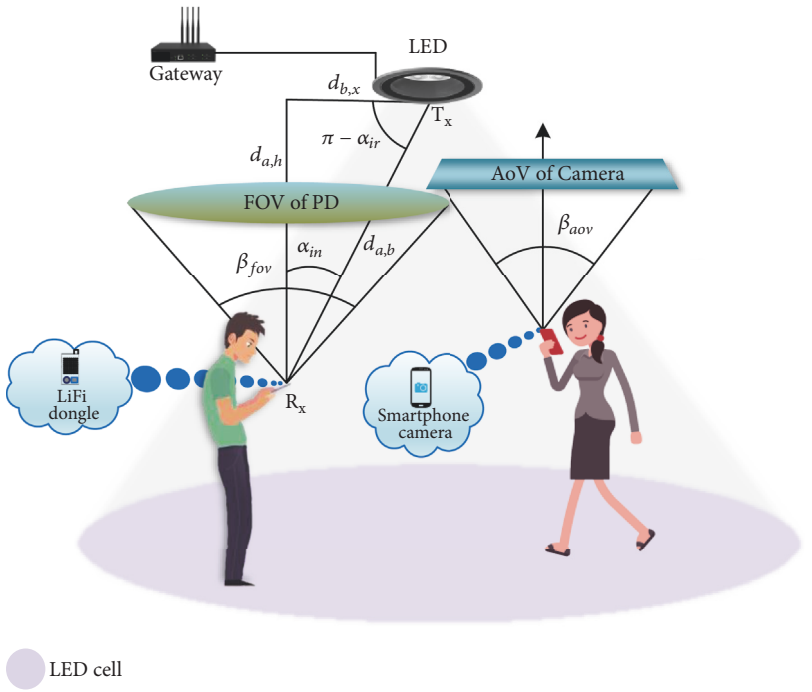

Figure 2: Data transmission model for the hybrid network.

where α_{in} implies the corresponding angle of incidence, g_{op} represents the gain of the optical filter, and Δ_{occ} is a rectangular function whose value implies that the channel has no gain if the LED remains outside of the angle-of-view (AoV) of camera receiver. If β_{aov} is the AoV of the camera, then Δ_{occ} is represented as

$$\Delta_{occ} = \begin{cases} 0, & \alpha_{in} \geq \beta_{aov} \\ 1, & \alpha_{in} < \beta_{aov} \end{cases} \tag{4}$$

A_c is the area of the entire image of the LED projected in the image sensor. It is often signified by the number of pixels occupied by the image. If ρ denotes the pixel edge length, then the projected area is

$$A_c = \frac{A_l {f_o}^2}{\rho^2 d_{a,b}^2} \tag{5}$$

where f_o denotes the focal length of the camera and A_l represents the physical area of the LED.

There is a minimum area of the projected image in the image sensor, below which the transmitted data cannot be decoded. The power received by the image sensor in this case is termed as the threshold power and expressed as

$$\begin{aligned} P_{th}^{IS} &= \arg\min P_r^{IS} \\ &= \arg\min \left[g_{op} \cos(\alpha_{in}) \Delta_{occ} \frac{R_o(\alpha) A_c P_t}{d_{a,b}^2} \right] \end{aligned} \tag{6}$$

where P_r^{IS} is the power received by the image sensor and P_t denotes the optical power transmitted by the LED.

Most existing commercial cameras offer a low AoV. As a result, the LOS components of neighboring LEDs do not reach inside the camera's AoV. Moreover, as mentioned above, introducing RoI signaling techniques significantly reduces the effect of the reflected components. Thus, OCC offers an excellent SINR, which is represented as

$$SINR_{occ} = \frac{\left(\zeta_c P_t H_{t,r}^{IS}\right)^2}{\sum_{i=0}^{N} \left(\zeta_c P_t H_{i,r}^{occ}\right)^2 + N_o f_r} \tag{7}$$

where ζ_c denotes the optical-to-electrical conversion efficiency at the image sensor, N_o is the spectral density of the

noise power, f_r is the sampling rate of the camera, N is the number of interfering transmitters, and $H_{i,r}^{occ}$ is the DC gain from these transmitters. The channel capacity can be expressed by the Shannon capacity formula [23], which is

$$C_{occ} = f_r W_s \log_2 \left(1 + SINR_{occ}\right) \tag{8}$$

where W_s represents the number of data symbols transmitted to the pixels within each image frame.

2.3. LiFi Channel Model. The NLOS part of the transmitted signal is disregarded in terms of LiFi because our baseband modulation bandwidth B is 20 MHz, which does not exceed the maximum allowable value [16, 39]. Thus, the LOS transmission model for LiFi is represented as

$$H_{t,r}^{PD} = g_{op} g_{con} \cos\left(\alpha_{in}\right) \Delta_{lifi} \frac{R_o\left(\alpha\right) A_p}{d_{a,b}^2} \tag{9}$$

where A_p denotes the physical area of the PD sensitive to light and g_{con} is the gain of the optical concentrator, which is a function of the refractive index and field-of-view (FoV) of PD. The rectangular function Δ_{lifi} is expressed as

$$\Delta_{lifi} = \begin{cases} 0, & \alpha_{in} \geq \beta_{fov} \\ 1, & \alpha_{in} < \beta_{fov} \end{cases} \tag{10}$$

where β_{fov} denotes the PD FoV. The PD should receive a certain amount of power to generate a minimum electrical current in order to decode the actual sent data bits. The threshold power of LiFi is denoted as

$$\begin{aligned} P_{th}^{PD} &= \arg\min P_r^{PD} \\ &= \arg\min \left[g_{op} g_{con} \cos\left(\alpha_{in}\right) \Delta_{lifi} \frac{R_o\left(\alpha\right) A_p P_t}{d_{a,b}^2} \right] \end{aligned} \tag{11}$$

where P_r^{PD} denotes the total amount of power received by the PD. LiFi uses an intensity based modulation scheme; as such, LiFi is affected by the interference generated by neighboring LEDs and other background lights. This interference ultimately results in reducing the SINR to a great extent, as LED infrastructures are commonly developed for indoor environments. Several studies [16, 40] have investigated the SINR in terms of LiFi, which can be expressed as

$$SINR_{lifi} = \frac{\left(\left(\zeta_p \sqrt{P_e}/P_t\right) P_t H_{t,r}^{PD}\right)^2}{\sum_{i=0}^{N} \left(\left(\zeta_p \sqrt{P_e}/P_t\right) P_t H_{i,r}^{PD}\right)^2 + N_o B} \tag{12}$$

where ζ_p is the optical-to-electrical conversion efficiency at the PD and P_e is the amount of electrical power converted after receiving the optical signals. The LiFi channel capacity can also be calculated from the Shannon capacity formula, which is

$$C_{lifi} = B \log_2 \left(1 + SINR_{lifi}\right) \tag{13}$$

3. FL-Based Network Assignment

Inside the hybrid network, the network is selected according to the type of service and quality that the user requires. FL is dispensed to assign a particular user to a network. Instead of making decisions for choosing a network in a hybrid system in terms of Boolean logic (only true or false values), the FL-based assignment considers truth values of variables ranging from 0 to 1 [33, 41–43]. We apply the Mamdani fuzzy inference system to evaluate our proposed scheme; this system includes three principal steps: fuzzification of input variables, rules evaluation, and defuzzification.

Fuzzification refers to the process of transforming the crisp inputs into degrees of functional blocks through using the different types of fuzzifiers, called membership functions. A fuzzy set is graphically represented by membership functions. For example, a triangular function is presented in Figure 3(a) and described as

$$\mu\left(x; a_T, b_T\right) = \begin{cases} 0, & x \leq a_T \ \ [Red\ line] \\ \dfrac{x - a_T}{b_T - a_T}, & a_T \leq x \leq b_T \ \ [Blue\ line] \\ 1, & x \geq b_T \ \ [Green\ line] \end{cases} \tag{14}$$

where a_T and b_T are the breakpoints of the membership functions and x is a particular input.

We considered four input variables to perform the network assignment mechanism: data rate requirement, SINR requirement, amount of instantaneous received power, and LOS Euclidean distance between the access point (AP) and the receiver. The variables are chosen on the basis of application scenarios. For example, if a user wants to localize its position, it will definitely need an excellent SINR rather than high data rate to minimize the localization resolution. On the contrary, both data rate and SINR must be high for a real-time video call. Moreover, the instantaneous power significantly contributes to determining the bit-error performance of connectivity. In addition, a low received power degrades the user's QoS level by increasing the outage probability to a great extent. On the other hand, the maximum communication distance varies for different optical wireless systems and user achieves satisfactory QoS when the communication distance is short. A long distance between the LED and receiver increases the interference for LiFi, although OCC is less affected by interference. In particular, the maximum communication distance for LiFi is very short compared to OCC for stable communications.

The membership functions are chosen on the basis of several experiments involving the use of training data. The grades of the membership functions are assigned according to the effect of variations in the value of a particular input. Figure 3(b) shows an illustration of the fuzzification of the SINR requirement of a specific user on the basis of service type and quality. The procedure is characterized by four different membership grades: low, average, high, and excellent. These grades are distributed from –10 to 60 dB. As shown in

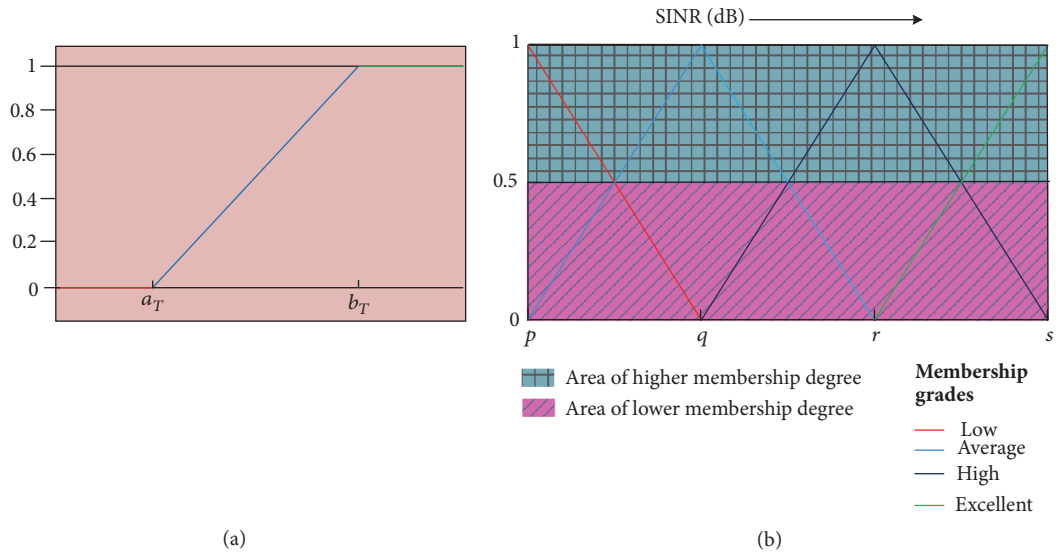

Figure 3: Fuzzification process: (a) a generalized triangular function; (b) SINR requirement.

Figure 3(b), the four membership grades can be represented in a similar approach, which is

$$\begin{aligned} Low &\longrightarrow \mu(x;p,q), \quad x \geq p \\ Average &\longrightarrow \begin{cases} 1-\mu(x;p,q), & x > p \\ \mu(x;q,r), & x \geq q \end{cases} \\ High &\longrightarrow \begin{cases} 1-\mu(x;q,r), & x > q \\ \mu(x;r,s), & x \geq r \end{cases} \\ Excellent &\longrightarrow 1-\mu(x;r,s), \quad x < s \end{aligned} \tag{15}$$

The chosen SINR values of the breakpoints are −10, 10, 30, and 40 dB. For example, if a user requires an SINR of around 25 dB, then the user will be categorized as "average" in the fuzzification process. Other inputs are fuzzified through a similar approach. However, the status of the membership grades is varied according to the numerical information of the input variables. For example, the data rate requirement is fuzzified through three membership grades: low, average, and high.

After fuzzifying the inputs, different rules are used to evaluate the performance of the hybrid system [41]. These if/then rules are generated by assigning a membership grade to each of the input variables, and a decision is made after multiplying (also can be referred to as "and" operation) the rules. For example, if the data rate requirement is low, the SINR requirement is excellent, and the instantaneous receive power is medium, then the user will be connected via LiFi for the shortest distance between the light source and receiver (or OCC for the highest distance). It is worth noting here that the rules are comprehensive and are generated keeping the nature and quality of the user requirements in mind. In general, rules are the guidelines generated according to the membership functions and serve as a basis for why we choose a particular network in a specific kind of service scenario.

The network assignment procedure is illustrated in Figure 4. The user must remain inside the LED cell in order to get connected via LiFi or OCC. However, the connection possibility significantly depends on the FoV or AoV offered by the PD or camera, respectively. Because the effects of the NLOS components on the optical signal are disregarded, the LED must appear inside the coverage area of the receiver. After getting a new network access request (NAR) from the user, the service type will be investigated. The examination on the input variables will be initiated immediately following the investigation. Then, the system will go through the fuzzification process described earlier.

Subsequently, the rules are employed and evaluated. The last stage of the network assignment mechanism is the mark allocation, a process that is also referred to defuzzification. The mark indicates the possibility of choosing a network in the network assignment process. Two separate outputs are considered for LiFi and OCC. Both outputs are characterized with triangular membership functions. We have considered five membership grades for each output to obtain a precise result in the network selection mechanism. In this paper, the mark is termed as network assignment factor (NAF) and denoted as ϑ_{lifi} and ϑ_{occ} for LiFi and OCC, respectively. We have adopted CoG [33] method for defuzzification because it shows better performance results than the bisector-of-area (BoA) method, which is realized through several experiments on training data. The NAF is provided as a crisp value by the CoG method, which is represented as

$$\begin{aligned} \text{For LiFi, } \vartheta_{lifi} &= \frac{\int_0^1 z\mu_l(z)\,dz}{\int_0^1 \mu_l(z)\,dz} \\ \text{For OCC, } \vartheta_{occ} &= \frac{\int_0^1 z\mu_c(z)\,dz}{\int_0^1 \mu_c(z)\,dz} \end{aligned} \tag{16}$$

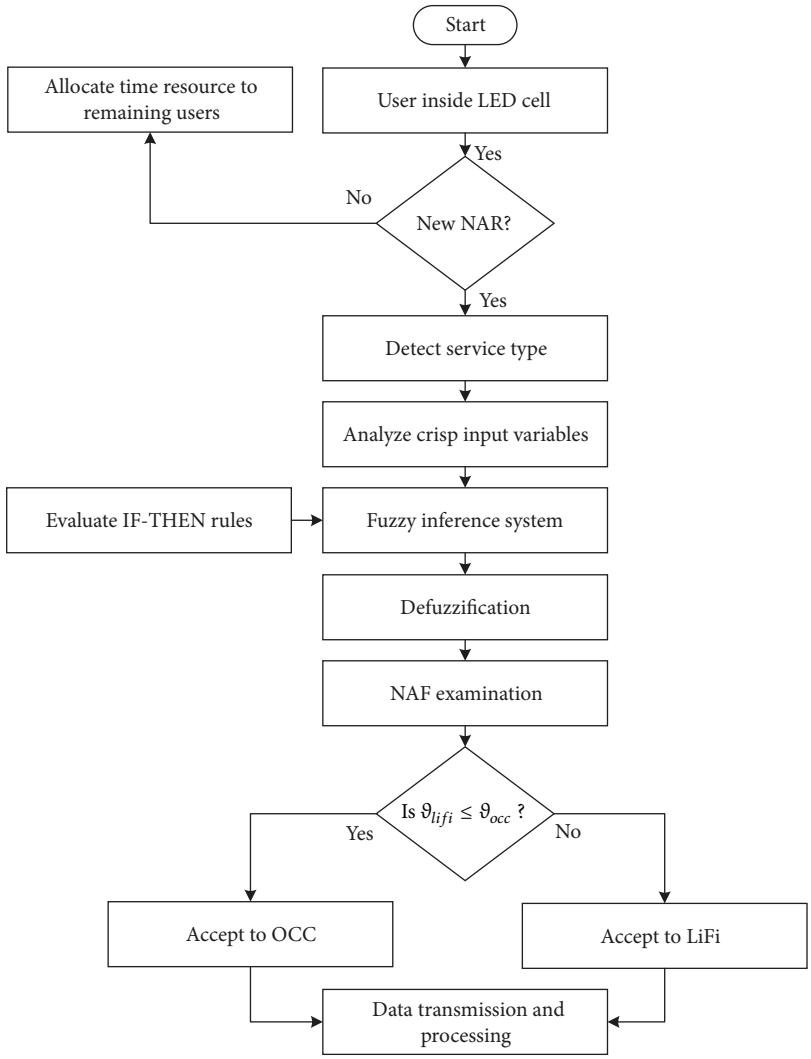

Figure 4: Admission strategy for a new network access request.

where $\int_0^1 \mu_I(z)dz$ indicates the total area of the region after combining all the membership functions. NAF values range from 0 to 1. In fact, a higher NAF increases the possibility of choosing a network. Thus, when a network access is requested by a new user, the NAFs of both networks will be compared. The network with the higher NAF will be chosen. For example, if LiFi achieves an NAF of 0.6 for a new user, whereas OCC obtains 0.8, then the user will be connected to OCC instead of LiFi.

When multiple users want to connect to the same AP and RRS [34], a TDMA technique is considered. Each user is allocated a particular time slot, referred to as quantum time, to ensure fairness among all users. If the process of serving the user is not entirely executed within that time slot, the process will resume after completing all other processes in the queue. Figure 5 illustrates an RRS scheduling process, in which four users want to get access from the serving light source. The process for LiFi user-2 does not finish within the allocated time slot, it gets connected again after the other time slots allocated in the queue have been completed.

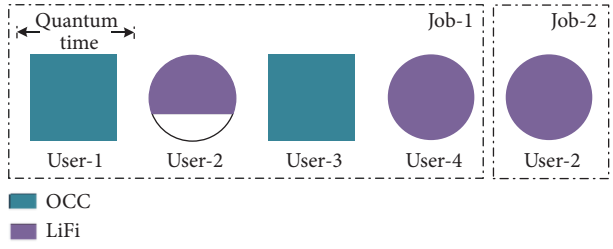

Figure 5: Example of RRS scheduling process.

The user QoS is measured considering achievable user data rate and SINR. We develop a parameter, referred as demand satisfaction factor (DSF), to analyze the QoS of users. If the user achieves a lower data rate or SINR than it requires, the DSF will be decreased. In general, DSF is calculated on the basis of time resource allocation to each user. The DSF of a particular user is represented as follows:

$$DSF = \begin{cases} \left(1 - \frac{n}{N_t}\right)\left(\frac{\lambda}{\sigma_i}\right)\frac{\varphi_{ai}\chi_{ai}}{\varphi_{ri}\chi_{ri}}, & \{\lambda < \sigma_i\} \,\&\, \{\varphi_{ai} < \varphi_{ri}\} \,\&\, \{\chi_{ai} < \chi_{ri}\} \\ \frac{\varphi_{ai}\chi_{ai}}{\varphi_{ri}\chi_{ri}}, & \{\lambda \geq \sigma_i\} \,\&\, \{\varphi_{ai} < \varphi_{ri}\} \,\&\, \{\chi_{ai} < \chi_{ri}\} \\ \frac{\chi_{ai}}{\chi_{ri}}, & \{\lambda \geq \sigma_i\} \,\&\, \{\varphi_{ai} \geq \varphi_{ri}\} \,\&\, \{\chi_{ai} < \chi_{ri}\} \\ \frac{\varphi_{ai}}{\varphi_{ri}}, & \{\lambda \geq \sigma_i\} \,\&\, \{\varphi_{ai} < \varphi_{ri}\} \,\&\, \{\chi_{ai} \geq \chi_{ri}\} \\ 1, & \{\lambda \geq \sigma_i\} \,\&\, \{\varphi_{ai} \geq \varphi_{ri}\} \,\&\, \{\chi_{ai} \geq \chi_{ri}\} \end{cases} \tag{17}$$

where φ_{ai} and φ_{ri} indicate the achievable and required data rate, respectively, and χ_{ai} and χ_{ri} indicate the achievable and required SINR, respectively. λ and σ_i represent the quantum time and burst time of the user, respectively. n indicates the total number of users waiting in queue at the particular time and N_t is the maximum number of users that can be connected inside the LED cell.

4. Link-Switching Strategy

It is already known that LiFi suffers from more interference than OCC. This interference can originate from the LOS component of other light sources or other components reflected from painted walls or mirrors. For simplicity, we assume an indoor scenario, in which a user can be connected to several LEDs. It is obvious that the user device will be affected by the LOS component of the neighboring LED near the edge of the LED cell. Thus, if just under the LED cell, the user will suffer the least amount of interference and will receive the best SINR. Therefore, the probability of allocation to the LiFi network will be high. If the user appears to be connected with OCC at that time, the probability of link-switching to LiFi will also be high because the final goal of network allocation is increasing the user QoS as much as possible. In the same way, if the user goes too close to the edge of the LED cell, then the probability of switching from a LiFi to an OCC network will be high. Figure 6 shows two LED cells, each having a diameter of ν. If γ% of the diameter of a specific LED cell is covered by a neighbor LED cell, the probability of user devices interfering with the neighbor LED within an LED cell will be

$$P_j = \sum_{j=1}^{\tau} \left[\frac{2\varepsilon \int_{(\nu - 2\gamma_j \nu)/2}^{\nu/2} \sqrt{\nu^2 - 4z^2}\, dz}{\tau \pi \nu^2} \right] \tag{18}$$

where ε is the total number of neighbor LED cells interfering with the serving LED cell and τ is the total number of user devices inside the cell. Thus, whenever the LOS distance between the LED AP and the receiver changes, the link-switching probability of either network will also be changed according to the user service requirements. The network assignment for the network switching request can be performed in two ways: LiFi-to-OCC and OCC-to-LiFi switching.

The link-switching can be implemented within either the same LED AP or different APs. Figure 7 shows the switching policy for OCC-to-LiFi. Initially, the user communicates using the OCC network. Then, the condition of the user will be investigated, i.e., whether the user is remaining static or roaming around the LED cells. The LOS distance from the LED AP to the camera will change for every microsecond for the moving user. Therefore, there will be chance for the camera to receive power below P_{th}^{IS}. In this case, communication between the user and LED AP will terminate. The immediate received power will be compared with P_{th}^{IS}, and when the power exceeds the threshold value, the LiFi received power will be immediately compared with P_{th}^{PD}. If the received power is higher than the threshold, then the user will be connected to LiFi. However, if the received power is also below threshold, the user will be connected to the adjacent AP and follow a new NAR strategy. There is a high possibility for a static user to switch between service and quality requirements. For example, the user can switch from 360p to 1080p video calling, or can stop real-time communication and start browsing. For this reason, whenever the user switches between different services, the NAF will be investigated. If NAF is found decreasing, then it will be compared to that of LiFi. If LiFi offers a higher NAF than OCC, then the user will be switched to LiFi. A similar strategy will be followed for LiFi-to-OCC switching, which is shown in Figure 8.

5. Network Switching Flow Process

In this section, we propose a detailed network switching flow mechanism for the hybrid system. The flow procedure is generalized and applicable to either OCC-to-LiFi or LiFi-to-OCC switching. The flow mechanism is illustrated in Figure 9.

The switching flow mechanism is implemented through 25 steps. When the user device senses that the NAF of the serving receiver (SR) is decreasing (step-1), it sends a report to the serving AP (SAP) it is connected to (step-2). The SR then searches for new signals (step-3), and the SAP by which the user will be connected to the target receiver (TR) is selected (step-4). Then the preauthentication is checked by the receiver with the target AP (TAP) (step-5). On the basis of the preauthentication and the NAF, the SR investigates the signal quality. Together, the SAP and SR decide if a switch to the TAP should be executed (step-6). The SAP initiates the switching process by sending a request to the TAP via a gateway (steps-7 and 8). Network assignment control (NAC) is initiated to specify the possibility of whether or not the network can be assigned (step-9). Afterward, the TAP responds to the switching request (steps-10 and 11). Then, a

Table 1: System parameters for the simulation.

Transmitter parameters	
LED radius	5 cm
Transmitted optical power, P_t	10 W
Half-intensity radiation angle, $\Psi_{1/2}$	60°
Gain of optical filter, g_{op}	1.0
LiFi parameters	
Physical area of PD	1 cm^2
Gain of optical concentrator, g_{con}	1.5
Optical-to-electrical conversion efficiency, ζ_p	0.53 A/W
Optical bandwidth, B	20 MHz
FoV, β_{fov}	85°
OCC parameters	
Image sensor size	6 × 4 (3:2 aspect ratio)
Pixel edge length, ρ	2 μm
Frame rate, f_r	30 fps
Focal length, f_o	6 mm
Optical-to-electrical conversion efficiency, ζ_c	0.51 A/W
AoV (diagonal), β_{aov}	60°

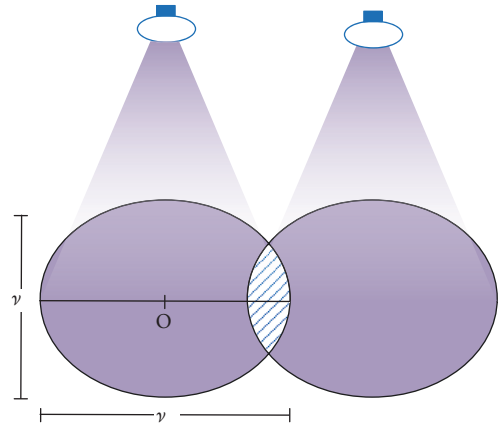

Figure 6: Illustration of two adjacent LED cells.

new link is set up between the TAP and gateway (steps-12 to 15), and eventually, packet data are forwarded to the TAP (step-16). An optical channel is reestablished with the TAP (step-17), reconfigured (steps-18 to 20) and finally detached from the SAP and synchronized with the TAP (step-21). The SR then sends a signal to the gateway, indicating the completion of the switching mechanism and synchronization with the TAP (steps-22 and 23). Finally, the optical link between the former SAP and gateway is deleted (steps-24 and 25), and the packets are sent to the TR via the TAP.

6. Performance Evaluation

In this section, the network assignment mechanism is simulated considering the system parameters summarized in Table 1. The hybrid system can be implemented in indoor and outdoor environments. OCC is particularly preferred in daylight, and both LiFi and OCC can be utilized during the nighttime. We performed the simulations while considering the maximum communication distance of LiFi and OCC. When the LOS distance is high, OCC is slightly more preferred than LiFi.

Figures 10 and 11 show how the NAFs vary with increasing communication distance for both LiFi and OCC. The considered fuzzy rules are arranged in Table 2. The simulations are particularly based on the different service scenarios of users. For example, in case a user wants to localize its position, the service does not need a high data rate; rather, it requires a least bit-error rate for precise localization. This case is considered in Scenario-A. A user who wants to browse websites is reflected in Scenario D. Scenarios B and C indicate high-quality voice and video calling users, and Scenarios E and F reflect the standard quality.

As shown in Figure 10, LiFi achieves an NAF higher than 0.5 when the communication distance is kept within 6 m in all cases. The main reason that LiFi works in a limited communication distance is because of the optical signal receiving characteristics of PDs. OCC provides a good NAF for all cases except high-quality voice and video calling users because of its data rate limitation, which is shown in Figure 11.

For mobility supporting characteristics of LiFi and OCC technologies, our proposed hybrid system also ensures efficient switching between networks based on the service scenarios. The switching is very essential, as the size of the LED cell is very small, and our current indoor environment is decorated with numerous LED infrastructures. Link-switching is initiated whenever the receive power of the serving network falls below the threshold value. Figure 12 illustrates the power received by the users from different distances from LED AP.

The link-switching probability of OCC and LiFi is illustrated in Figure 13. The probability is measured considering

Table 2: Selected fuzzy rules for different scenarios.

Scenarios	Req. data rate	Req. SINR	Ins. receive power
A	Low	Excellent	Medium
B	Average	High	High
C	High	Excellent	High
D	Average	Poor	Low
E	Average	Average	High
F	Average	High	High

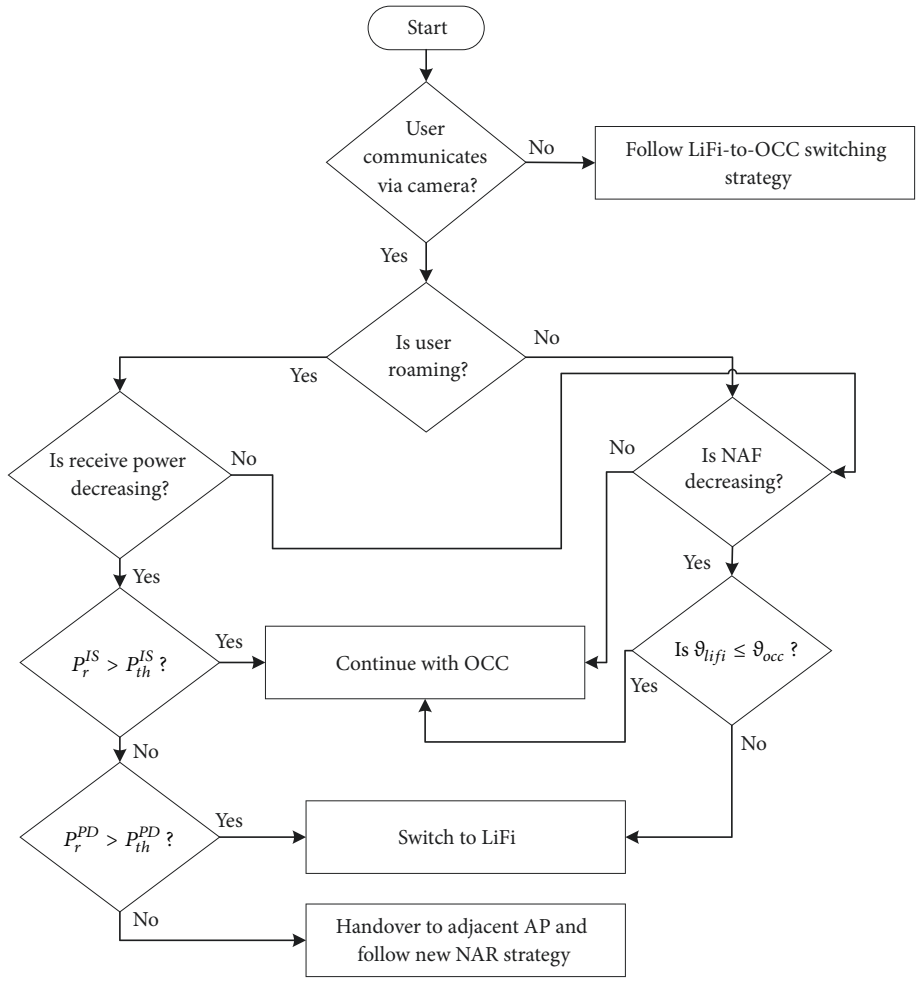

Figure 7: OCC-to-LiFi link-switching strategy.

an indoor scenario in which the diameter of the LED cell is 10 m. The link-switching probability is illustrated in terms of probability of user position inside the LED cell to receive highest optical signal. The highest position probability inside the LED cell corresponds with a user situated at the center of the LED cell (represented by O in Figure 6), and the lowest probability corresponds with a user located at the edge of the LED cell. It can be seen in Figure 13 that a user has a high probability of switching from LiFi-to-OCC when it remains near the LED cell origin. However, the probability decreases whenever the user comes close to the LED cell of the neighboring LED. The OCC-to-LiFi handover probability attains the inverse situation because of the capability of the camera to spatially separate the interfering element from the image sensor.

Figure 14 illustrates the outage probability of our proposed hybrid scheme. We set the threshold of the LiFi SINR as 0 dB for the simulation. We can clearly see that the outage probability is higher when the user moves away from the AP in terms of using LiFi only. However, after integrating OCC and LiFi, a clear improvement in outage possibility can be observed. The QoS performance of users is presented in Figure 15. The average DSF is measured assuming 0.16 persons/meter^2 can be served inside the LED

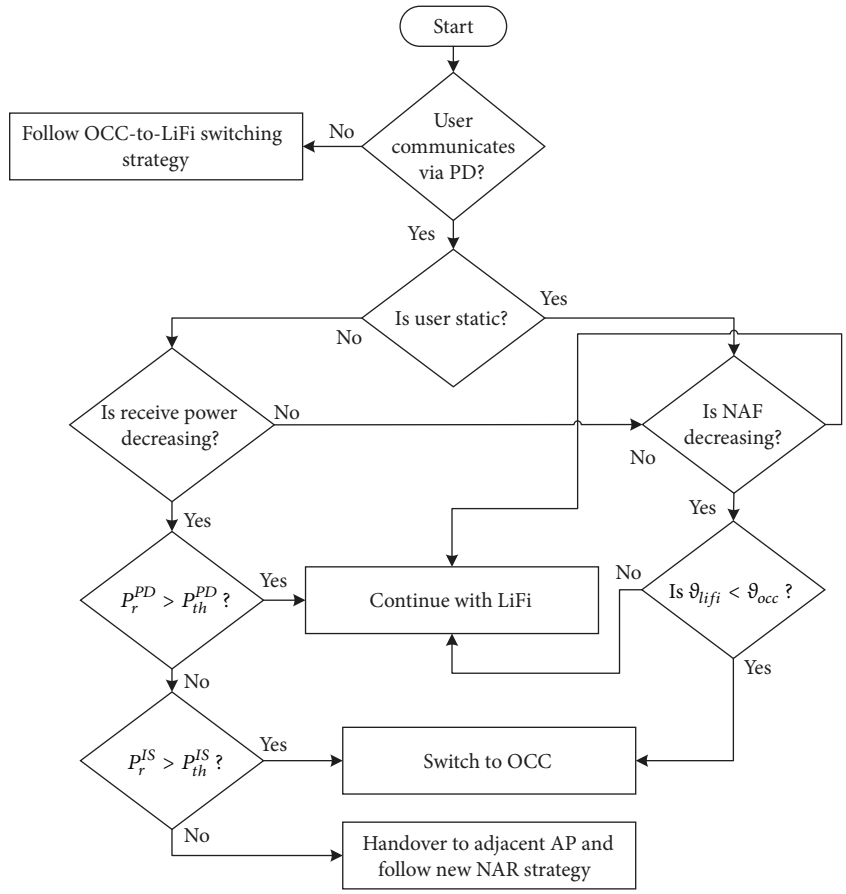

Figure 8: LiFi-to-OCC link-switching strategy.

cell. We also assume the number of users connected to OCC and LiFi in the hybrid infrastructure are same. Although the performance greatly depends on how much time is allocated to each user, our proposed scheme demonstrates better QoS performance than the case when only LiFi is present.

7. Conclusions

Next generation VLC networks will be exploited to achieve a higher service quality for users in all kinds of environments. One of the main advantages of using VLC is that existing lighting infrastructures can be utilized to send data to users. LiFi is a OWC technology that offers a high data rate. However, it suffers from interferences when there are multiple light sources, and the interference originated from these sources eventually degrades the service quality. Using OCC, the SINR can be significantly improved in all kinds of scenarios. Thus, the combination of high data rate and high SINR can be achieved by integrating OCC and LiFi. A hybrid OCC and LiFi architecture is proposed in this paper in which the network assignment for each user is based on FL. By using the FL concept, optimality can be achieved with less computational complexity. After defuzzification, each network generates a score called NAF, which is utilized to assign the appropriate network to a particular user. Furthermore, a link-switching mechanism based on FL is proposed, and a network switching flow analysis is provided. Performance is evaluated on the basis of different practical scenarios, and this evaluation includes switching and outage probability analysis inside the LED cell. The user QoS is also analyzed, and the results of this analysis demonstrate the importance of our proposed scheme.

8. Future Research

Currently, researchers are working on enabling the coexistence of RF and OWC to achieve high-data-rate output with improved coverage. The coexistence of different OWC technologies for the same kind of AP can be utilized to achieve a better service quality for users. The implementation of our proposed hybrid system in different application scenarios will be a momentous topic in future OWC related research, which will include testing our system's optimality with respect to other future homogenous hybrid infrastructures.

Data Availability

The data used to support the findings of this study are available from the corresponding author upon request.

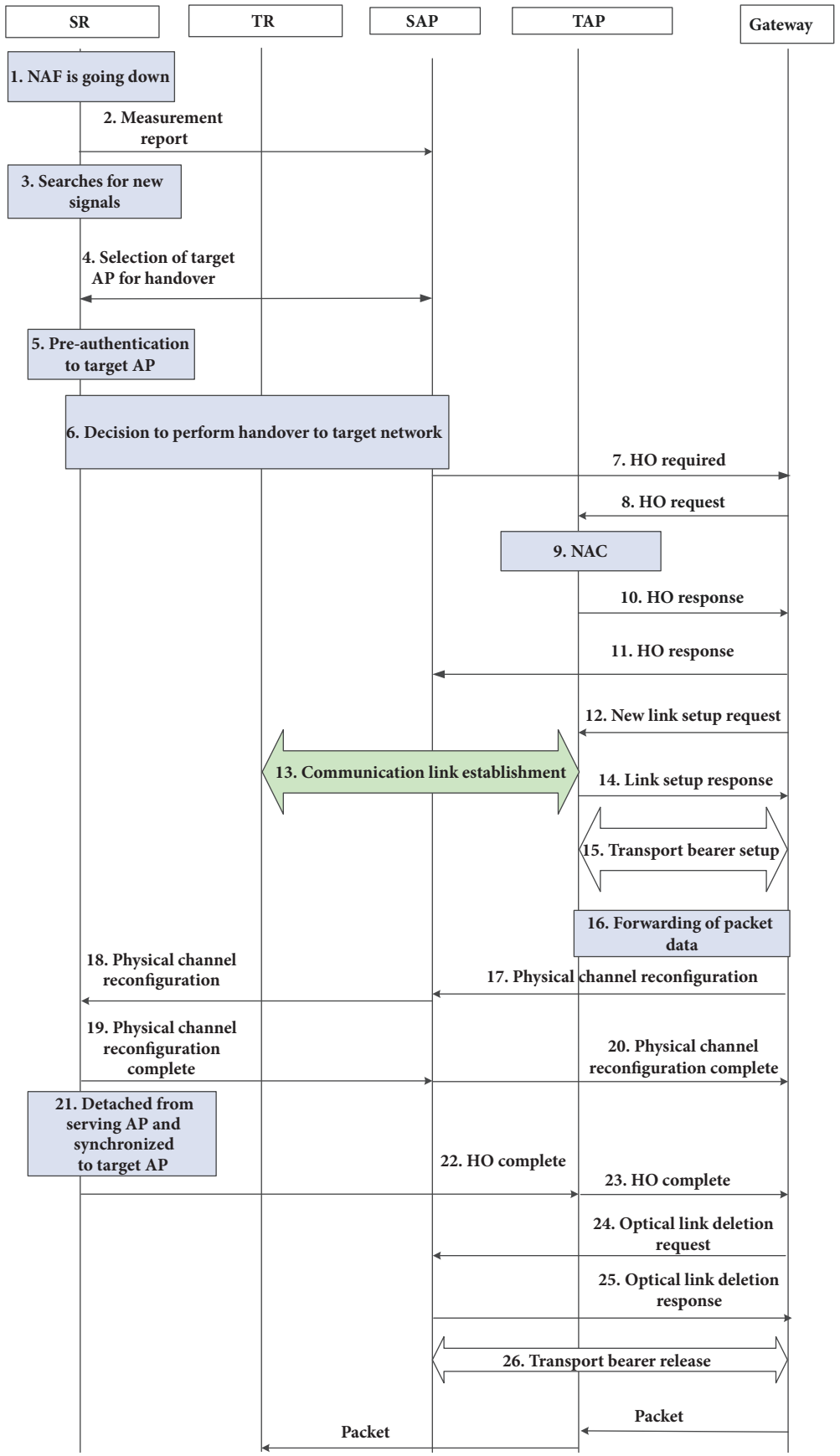

Figure 9: Network switching flow strategy.

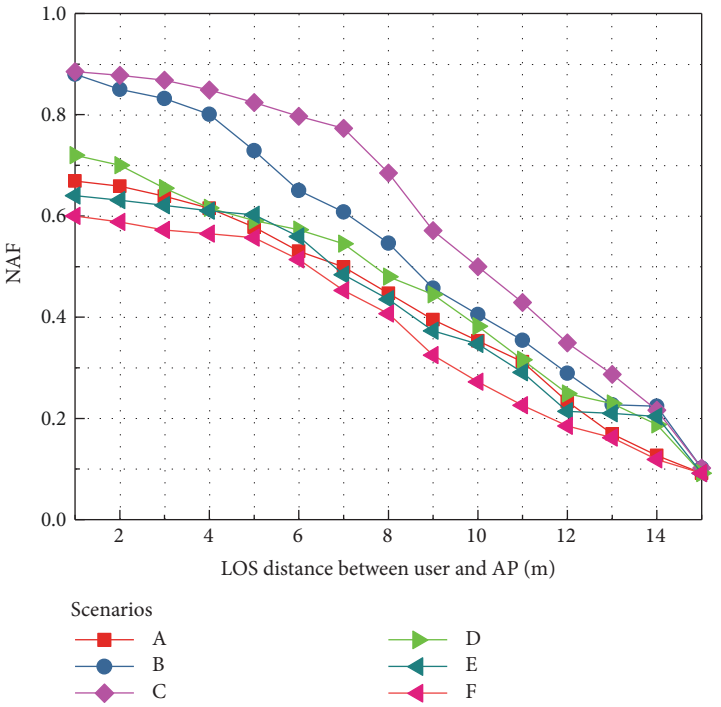

Figure 10: NAF variation using LiFi with increasing distance between user and LED AP.

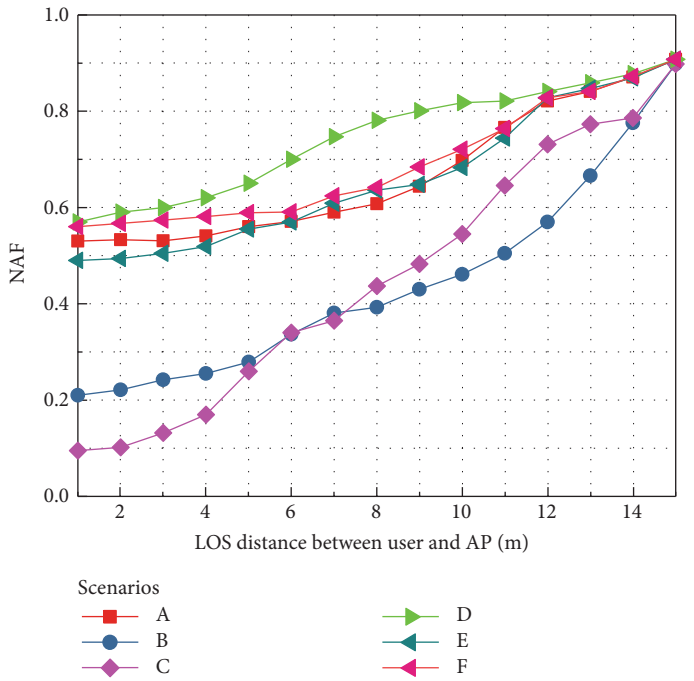

Figure 11: NAF variation using OCC with increasing distance between user and LED AP.

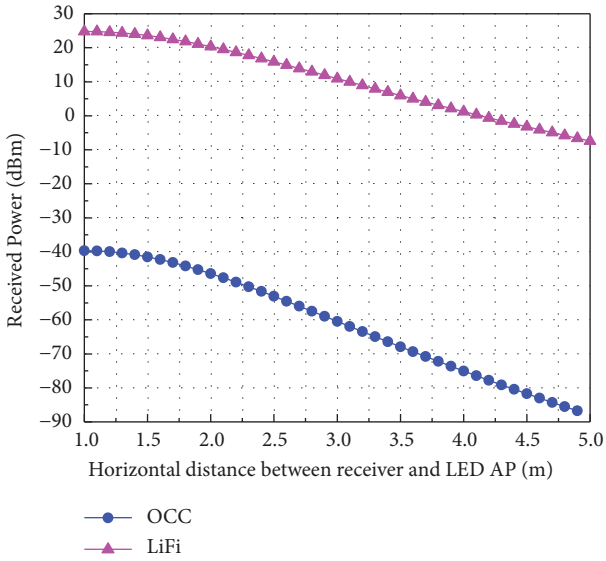

Figure 12: Distribution of received power for LiFi and OCC.

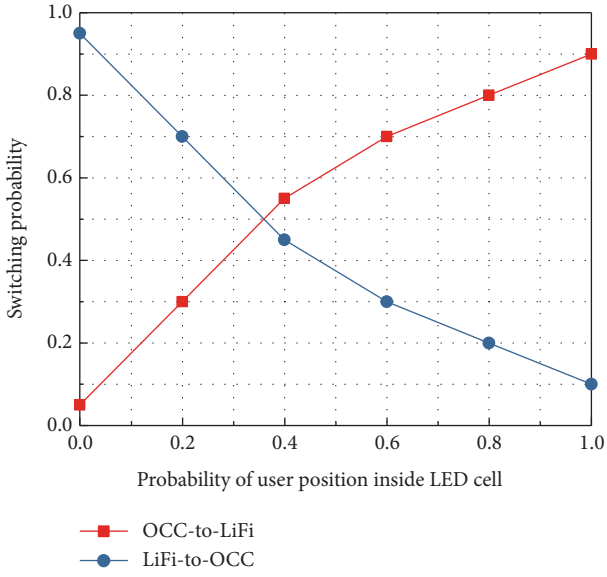

Figure 13: Link-switching probability analysis.

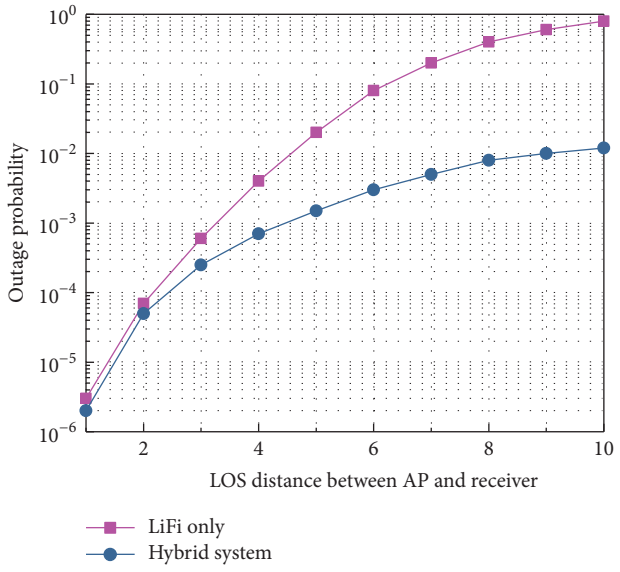

Figure 14: Comparison of outage probability.

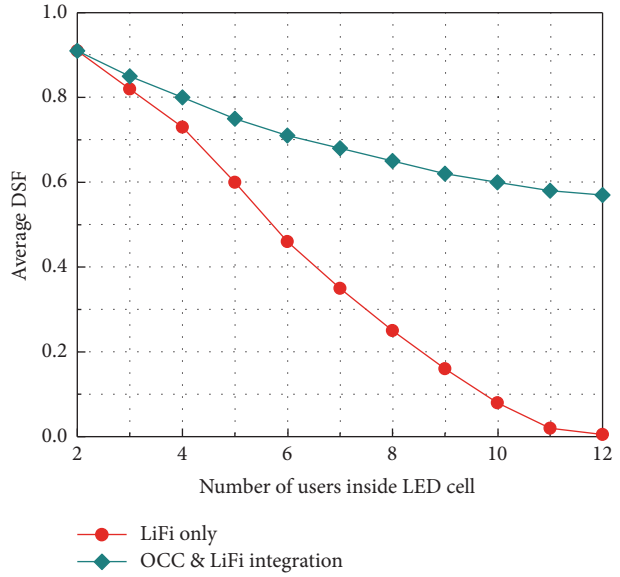

Figure 15: Average DSF comparison for multiple users served by the same LED AP.

Disclosure

This article is an extended version of a paper presented in the International Conference on Ubiquitous and Future Networks (ICUFN 2018), Prague, Czech Republic, July 2018.

Conflicts of Interest

The authors do not have any conflicts of interest.

Acknowledgments

This work was supported by Institute for Information & Communications Technology Promotion (IITP) grant funded by the Korea Government (MSIT) (no. 2017-0-00824, Development of Intelligent and Hybrid OCC-LiFi Systems for Next Generation Optical Wireless Communications).

References

[1] Z. Ghassemlooy, S. Arnon, M. Uysal, Z. Xu, and J. Cheng, "Emerging Optical Wireless Communications-Advances and Challenges," *IEEE Journal on Selected Areas in Communications*, vol. 33, no. 9, pp. 1738–1749, 2015.

[2] P. H. Pathak, X. Feng, P. Hu, and P. Mohapatra, "Visible Light Communication, Networking, and Sensing: A Survey, Potential and Challenges," *IEEE Communications Surveys & Tutorials*, vol. 17, no. 4, pp. 2047–2077, 2015.

[3] M. Z. Chowdhury, M. T. Hossan, A. Islam, and Y. M. Jang, "A Comparative Survey of Optical Wireless Technologies: Architectures and Applications," *IEEE Access*, vol. 6, pp. 9819–9840, 2018.

[4] H. Chen, H. P. A. Van Den Boom, E. Tangdiongga, and T. Koonen, "30-Gb/s bidirectional transparent optical transmission with an MMF access and an indoor optical wireless link," *IEEE Photonics Technology Letters*, vol. 24, no. 7, pp. 572–574, 2012.

[5] D. K. Borah, A. C. Boucouvalas, C. C. Davis, S. Hranilovic, and K. Yiannopoulos, "A review of communication-oriented optical wireless systems," *EURASIP Journal on Wireless Communications and Networking*, vol. 91, pp. 1–28, 2012.

[6] H. Elgala, R. Mesleh, and H. Haas, "Indoor optical wireless communication: Potential and state-of-the-art," *IEEE Communications Magazine*, vol. 49, no. 9, pp. 56–62, 2011.

[7] D. Karunatilaka, F. Zafar, V. Kalavally, and R. Parthiban, "LED based indoor visible light communications: state of the art," *IEEE Communications Surveys & Tutorials*, vol. 17, no. 3, pp. 1649–1678, 2015.

[8] R. Zhang, J. Wang, Z. Wang, Z. Xu, C. Zhao, and L. Hanzo, "Visible light communications in heterogeneous networks: Paving the way for user-centric design," *IEEE Wireless Communications Magazine*, vol. 22, no. 2, pp. 8–16, 2015.

[9] A. C. Boucouvalas, P. Chatzimisios, Z. Ghassemlooy, M. Uysal, and K. Yiannopoulos, "Standards for indoor Optical Wireless Communications," *IEEE Communications Magazine*, vol. 53, no. 3, pp. 24–31, 2015.

[10] M. Leba, S. Riurean, and A. Lonica, "LiFi - The path to a new way of communication," in *Proceedings of the 12th Iberian Conference on Information Systems and Technologies, CISTI 2017*, Portugal, June 2017.

[11] Y. Perwej, "The Next Generation of Wireless Communication Using Li-Fi (Light Fidelity) Technology," *Computer Networks*, vol. 4, no. 1, pp. 20–29, 2017.

[12] Y. Wang, X. Wu, and H. Haas, "Load Balancing Game with Shadowing Effect for Indoor Hybrid LiFi/RF Networks," *IEEE Transactions on Wireless Communications*, vol. 16, no. 4, pp. 2366–2378, 2017.

[13] M. Kashef, M. Ismail, M. Abdallah, K. A. Qaraqe, and E. Serpedin, "Energy efficient resource allocation for mixed RF/VLC heterogeneous wireless networks," *IEEE Journal on Selected Areas in Communications*, vol. 34, no. 4, pp. 883–893, 2016.

[14] F. Jin, R. Zhang, and L. Hanzo, "Resource allocation under delay-guarantee constraints for heterogeneous visible-light and RF femtocell," *IEEE Transactions on Wireless Communications*, vol. 14, no. 2, pp. 1020–1034, 2015.

[15] Y. Wang, D. A. Basnayaka, X. Wu, and H. Haas, "Optimization of Load Balancing in Hybrid LiFi/RF Networks," *IEEE Transactions on Communications*, vol. 65, no. 4, pp. 1708–1720, 2017.

[16] Y. Wang and H. Haas, "Dynamic Load Balancing with Handover in Hybrid Li-Fi and Wi-Fi Networks," *Journal of Lightwave Technology*, vol. 33, no. 22, pp. 4671–4682, 2015.

[17] M. Ayyash, H. Elgala, A. Khreishah et al., "Coexistence of WiFi and LiFi toward 5G: concepts, opportunities, and challenges," *IEEE Communications Magazine*, vol. 54, no. 2, pp. 64–71, 2016.

[18] G. Pan, J. Ye, and Z. Ding, "Secure Hybrid VLC-RF Systems with Light Energy Harvesting," *IEEE Transactions on Communications*, vol. 65, no. 10, pp. 4348–4359, 2017.

[19] S. Shao and A. Khreishah, "Delay Analysis of Unsaturated Heterogeneous Omnidirectional-Directional Small Cell Wireless Networks: The Case of RF-VLC Coexistence," *IEEE Transactions on Wireless Communications*, vol. 15, no. 12, pp. 8406–8421, 2016.

[20] H.-S. Kim, D.-H. Kwon, S.-H. Yang, Y.-H. Son, and S.-K. Han, "Channel assignment technique for RF frequency reuse in CA-VLC-based accurate optical indoor localization," *Journal of Lightwave Technology*, vol. 32, no. 14, pp. 2544–2555, 2014.

[21] P. Luo, Z. Ghassemlooy, H. Le Minh, X. Tang, and H.-M. Tsai, "Undersampled phase shift ON-OFF keying for camera communication," in *Proceedings of the 6th International Conference on Wireless Communications and Signal Processing (WCSP '14)*, pp. 1–6, IEEE, Hefei, China, October 2014.

[22] T. Yamazato, I. Takai, H. Okada et al., "Image-sensor-based visible light communication for automotive applications," *IEEE Communications Magazine*, vol. 52, no. 7, pp. 88–97, 2014.

[23] T. Nguyen, A. Islam, T. Hossan, and Y. M. Jang, "Current status and performance analysis of optical camera communication technologies for 5G networks," *IEEE Access*, vol. 5, pp. 4574–4594, 2017.

[24] Y. Goto, I. Takai, T. Yamazato et al., "A New Automotive VLC System Using Optical Communication Image Sensor," *IEEE Photonics Journal*, vol. 8, no. 3, pp. 1–17, 2016.

[25] R. D. Roberts, "Undersampled frequency shift ON-OFF keying (UFSOOK) for camera communications (CamCom)," in *Proceedings of the 22nd Wireless and Optical Communications Conference, WOCC '13*, pp. 645–648, China, May 2013.

[26] I. Takai, S. Ito, K. Yasutomi, K. Kagawa, M. Andoh, and S. Kawahito, "LED and CMOS image sensor based optical wireless communication system for automotive applications," *IEEE Photonics Journal*, vol. 5, no. 5, 2013.

[27] M. T. Hossan, M. Z. Chowdhury, A. Islam, and Y. M. Jang, "A Novel Indoor Mobile Localization System Based on Optical Camera Communication," *Wireless Communications and Mobile Computing*, vol. 2018, 17 pages, 2018.

[28] B. Lin, Z. Ghassemlooy, C. Lin, X. Tang, Y. Li, and S. Zhang, "An Indoor Visible Light Positioning System Based on Optical Camera Communications," *IEEE Photonics Technology Letters*, vol. 29, no. 7, pp. 579–582, 2017.

[29] T. Nguyen, A. Islam, T. Yamazato, and Y. M. Jang, "Technical Issues on IEEE 802.15.7m Image Sensor Communication Standardization," *IEEE Communications Magazine*, vol. 56, no. 2, pp. 213–218, 2018.

[30] I. Takai, T. Harada, M. Andoh, K. Yasutomi, K. Kagawa, and S. Kawahito, "Optical vehicle-to-vehicle communication system using LED transmitter and camera receiver," *IEEE Photonics Journal*, vol. 6, no. 5, pp. 1–14, 2014.

[31] T. Yamazato, M. Kinoshita, S. Arai et al., "Vehicle Motion and Pixel Illumination Modeling for Image Sensor Based Visible Light Communication," *IEEE Journal on Selected Areas in Communications*, vol. 33, no. 9, pp. 1793–1805, 2015.

[32] P. Ji, H.-M. Tsai, C. Wang, and F.-Q. Liu, "Vehicular visible light communications with led taillight and rolling shutter camera," in *Proceedings of the IEEE 79th Vehicular Technology Conference (VTC '14)*, pp. 1–6, Seoul, Republic of Korea, May 2014.

[33] T. J. Ross, *Fuzzy Logic with Engineering Applications*, John Wiley & Sons, Ltd, 3rd edition, 2011.

[34] M. Kawser, "Performance Comparison between Round Robin andProportional Fair Scheduling Methods for LTE," *International Journal of Information and Electronics Engineering*, vol. 2, no. 5, pp. 678–681, 2012.

[35] P. Luo, M. Zhang, Z. Ghassemlooy, S. Zvanovec, S. Feng, and P. Zhang, "Undersampled-Based Modulation Schemes for Optical Camera Communications," *IEEE Communications Magazine*, vol. 56, no. 2, pp. 204–212, 2018.

[36] R. D. Roberts, "A MIMO protocol for camera communications (CamCom) using undersampled frequency shift ON-OFF keying (UFSOOK)," in *Proceedings of the IEEE Globecom Workshops (GC Wkshps '13)*, pp. 1052–1057, Atlanta, GA, December 2013.

[37] P. Luo et al., "Experimental demonstration of RGB LED-based optical camera communications," *IEEE Photonics Journal*, vol. 7, no. 5, pp. 1–12, 2015.

[38] J. M. Kahn and J. R. Barry, "Wireless infrared communications," *Proceedings of the IEEE*, vol. 85, no. 2, pp. 265–298, 1997.

[39] V. Jungnickel, V. Pohl, S. Nönnig, and C. Von Helmolt, "A physical model of the wireless infrared communication channel," *IEEE Journal on Selected Areas in Communications*, vol. 20, no. 3, pp. 631–640, 2002.

[40] X. Wu, M. Safari, and H. Haas, "Access Point Selection for Hybrid Li-Fi and Wi-Fi Networks," *IEEE Transactions on Communications*, vol. 65, no. 12, pp. 5375–5385, 2017.

[41] M. Kaya and R. Alhajj, "Utilizing genetic algorithms to optimize membership functions for fuzzy weighted association rules mining," *Applied Intelligence*, vol. 24, no. 1, pp. 7–15, 2006.

[42] T. Bouali and S. Senouci, "A fuzzy logic-based communication medium selection for QoS preservation in vehicular networks," in *Proceedings of the IEEE International Conference on Communications (ICC '16)*, pp. 1–6, Kuala Lumpur, Malaysia, May 2016.

[43] A. I. Aziz, S. Rizvi, and N. M. Saad, "Fuzzy logic based vertical handover algorithm between LTE and WLAN," in *Proceedings of the International Conference on Intelligent and Advanced Systems (ICIAS '10)*, pp. 1–4, IEEE, Kuala Lumpur, Malaysia, June 2010.